

Non-intrusive appliance health monitoring and remaining useful life prediction using a DRN-transformer model

Xihuan Su¹, Antonette Villapando Chua², Anton Louise De Ocampo³,
Ralph Gerard B. Sangalang⁴, Oliver Lexter July A. Jose⁵, Dianyou Kang⁶
College of Engineering, Batangas State University the National Engineering University,
Alangilan Campus, Batangas City 4200, Philippines

²Corresponding author

E-mail: ¹22-09293@g.batstate-u.edu.ph, ²antonette.chua@g.batstate-u.edu.ph,
³antonlouise.deocampo@g.batstate-u.edu.ph, ⁴ralphgerard.sangalang@g.batstate-u.edu.ph,
⁵oliverlexerjuly.jose@g.batstate-u.edu.ph, ⁶22-08073@g.batstate-u.edu.ph

Received 13 October 2025; accepted 22 March 2026; published online 15 May 2026
DOI <https://doi.org/10.21595/mme.2026.25565>



Copyright © 2026 Xihuan Su, et al. This is an open access article distributed under the Creative Commons Attribution License, which permits unrestricted use, distribution, and reproduction in any medium, provided the original work is properly cited.

Abstract. This paper presents a high-performance embedded micro-sensing and processing integrated non-intrusive load monitoring system for real-time appliance health assessment and remaining useful life (RUL) prediction, with the core innovation focused on the design and implementation of an STM32H7-based embedded micro-system that realizes seamless integration of high-frequency signal acquisition, edge-side real-time preprocessing, and intelligent multi-task analysis on a single chip. Utilizing an STM32H7 microcontroller, it captures high-frequency voltage and current signals to detect appliance degradation features. Time-frequency preprocessing with FFT and STFT improves signal representation, enabling better feature extraction. The proposed DRN-Transformer model integrates deep residual networks and Transformer attention mechanisms to extract both local and long-range temporal features. Tested on four common household appliances (refrigerator, washing machine, air conditioner, microwave oven), the system achieved over 92 % accuracy in health classification (up to 97.8 % for washing machines) and a low error in RUL estimation with an average RMSE of 3.2 months and an average MAPE of 8.5 %, outperforming traditional machine learning baselines (SVM/RF) by more than 40 % in health classification accuracy and surpassing mainstream deep learning models (LSTM/Transformer/LSTM-VMD) by 15-20 % in RUL prediction precision. Furthermore, the proposed embedded micro-sensing platform explicitly considers hardware-level constraints such as on-chip memory capacity, computational complexity, and real-time inference latency. By optimizing model architecture and adopting lightweight deployment strategies, the system achieves efficient edge-side intelligence while maintaining compatibility with resource-constrained microcontroller platforms. The system outperformed traditional baseline models and showed good generalization across different brands. With low latency and power consumption, it is well-suited for smart home applications.

Keywords: non-intrusive load monitoring, DRN-transformer, appliance health assessment, embedded micro-sensing system.

1. Introduction

The evolution of smart home technologies, the proliferation of IoT devices, and the growing demand for energy-efficient management have intensified the need for intelligent systems capable of assessing appliance performance and predicting potential failures [1]. In particular, the ability to non-invasively monitor appliances' health status and anticipate end-of-life events has become increasingly vital in reducing maintenance costs, preventing unexpected breakdowns, and enhancing overall energy usage efficiency [2].

Traditional appliance monitoring approaches often rely on intrusive sensors that require

installation within each individual device. These methods are costly, complex, and lack scalability, especially in residential environments with diverse appliances. Non-intrusive load monitoring (NILM) addresses these limitations by analyzing aggregate electrical signals – such as voltage and current – from a single point of measurement, such as a smart meter. Through pattern recognition and signal disaggregation, NILM enables the identification of specific appliances' operational states without physical intervention [3]. From the perspective of embedded microsystem engineering, intelligent sensing platforms must simultaneously satisfy constraints in power consumption, memory footprint, computational efficiency, and real-time processing capability. In practical smart home deployments, NILM algorithms are often expected to operate directly on embedded hardware such as microcontrollers rather than high-performance servers. Therefore, the co-design of sensing hardware, signal processing pipelines, and lightweight deep learning models becomes critical for achieving reliable real-time monitoring in resource-constrained environments.

Despite its promise, NILM technology still faces significant challenges. Signal noise, overlapping appliance activity, and insufficient real-time capability hinder accurate state identification and degrade prediction performance. Furthermore, most existing solutions are either constrained by limited hardware performance or rely on traditional machine learning algorithms that struggle with complex temporal dynamics.

To overcome these obstacles, this study proposes a novel NILM system that integrates a high-frequency embedded sensing platform based on an STM32 microcontroller and a hybrid deep learning model named DRN-Transformer [4]. The STM32H7 MCU provides a 1 MHz sampling rate, which is essential for capturing short-duration transients and high-frequency harmonics indicative of early appliance degradation. The DRN-Transformer architecture combines the strengths of deep residual networks (DRN) in local feature learning and transformer mechanisms in long-range temporal modeling. This fusion allows for enhanced state classification accuracy and robust estimation of remaining useful life (RUL).

Additionally, the proposed system introduces a preprocessing pipeline incorporating time-frequency transformation techniques such as Fast Fourier Transform (FFT) and Short-Time Fourier Transform (STFT). These methods enhance signal clarity by extracting both global periodic and local transient features, making the model more resilient to noise and capable of recognizing subtle degradation patterns [5]. The objectives and contributions of this paper can be summarized as follows: With the rapid development of embedded intelligence, micro-scale machinery monitoring increasingly demands compact, low-power, and high-reliability sensing and computing platforms [18-20]. However, existing NILM and smart metering solutions struggle to simultaneously support high-frequency sampling, real-time processing, and resource-efficient deployment, which highlights the necessity and significance of the proposed embedded DRN-Transformer framework. Development of a cost-efficient, embedded smart meter platform using STM32H7 capable of high-resolution load data acquisition. Implementation of a hybrid DRN-Transformer deep learning model tailored for dual tasks: health classification and RUL prediction. Enhancement of signal interpretability through time-frequency feature engineering using FFT and STFT. Extensive experimentation on four commonly used household appliances – refrigerator, washing machine, air conditioner, microwave oven – demonstrating the system's effectiveness, adaptability across brands, and real-time performance [6].

This paper is organized as follows. Section 2 reviews relevant literature on NILM methodologies, deep learning in appliance monitoring, and STM32-based data acquisition systems. Section 3 describes the architecture of the proposed system, including hardware, preprocessing, and model design. Section 4 presents experimental settings and performance evaluations. Section 5 discusses technical implications and limitations. Section 6 concludes with a summary and future research directions.

2. Related review

This section reviews the relevant research on non-intrusive load monitoring (NILM) from two independent perspectives: AI-based NILM modeling for health assessment and RUL prediction, and embedded micro-system implementation for NILM applications, and further compares the research status of existing embedded NILM hardware platforms, clarifying the system-level innovation of the proposed embedded micro-sensing platform in this paper. Recent advances in non-intrusive load monitoring (NILM), deep learning applications in energy systems, and embedded smart metering have paved the way for more sophisticated appliance health assessment systems [7]. This section reviews the most relevant works categorized by their technical contributions.

Xu compared empirical mode decomposition (EMD) and wavelet decomposition for multi-scale signal analysis, demonstrating the superiority of EMD in identifying subtle load variations [8]. Their results laid a foundation for signal preprocessing in NILM systems. Similarly, Jrhilifa proposed a bivariate EMD-based denoising method that improved robustness in handling non-stationary signals, essential for accurate appliance state classification [9].

Several studies have employed deep neural networks for power load recognition and prediction. For instance, Padder utilized data-driven models for acoustic signature-based health monitoring, emphasizing the capability of deep learning to detect minute operational anomalies [10]. Wu proposed a Transformer-BiLSTM hybrid for smart meter anomaly detection, which developed a spatiotemporal graph neural network to forecast post-disturbance frequency in power grids, illustrating the feasibility of graph-based and attention-enhanced models in time-series forecasting tasks [11].

STM32 microcontrollers have gained prominence in NILM applications due to their high-speed ADCs, low power consumption, and robust interfacing capabilities. Young highlighted STM32 multi-channel synchronous acquisition and real-time processing strengths in complex load environments [12]. Thirunavukkarasu emphasized STM32 energy efficiency, making it suitable for long-term deployment in residential systems [13].

Preprocessing plays a vital role in improving model performance. Khalil showed that deep learning models outperform statistical methods in handling nonlinear, non-stationary time-series [14]. Kumar incorporated Fourier and wavelet-based feature enhancement to improve model accuracy and generalization [15]. Furthermore, Anwar demonstrated the benefit of using signal decomposition techniques like VMD and EMD in boosting prediction accuracy for power and health metrics [16].

The literature supports the effectiveness of deep learning and embedded hardware in NILM applications. Existing embedded NILM platforms typically rely on low-frequency sampling smart meters or edge gateways with limited signal processing capability. Many studies focus primarily on algorithmic improvements while overlooking hardware–software co-design and real-time deployment feasibility. Compared with these approaches, the proposed system integrates high-frequency sensing, on-device signal preprocessing, and lightweight deep learning inference within a single embedded microcontroller platform. This integrated design significantly improves real-time capability and system compactness, making it more suitable for distributed smart sensing environments. However, gaps remain in real-time, multi-brand adaptation and lifetime prediction [17]. This paper addresses these challenges by combining time-frequency signal processing, transfer learning, and a hybrid DRN-Transformer model on a low-cost, high-performance STM32 platform. Kannimuthu et al. [18] enhanced watershed segmentation for medical image detection by integrating feedforward neural networks, highlighting the ability of neural models to refine feature boundaries and improve classification precision in noisy environments. Although applied to mammogram analysis, their methodology underscores the general effectiveness of neural architectures in extracting discriminative features from high-dimensional data. From a system-level perspective, Dheer et al. [19] investigated security and reliability considerations in interactive communication media algorithms, emphasizing robustness, stability, and trustworthy

data transmission in networked intelligent systems. These considerations are closely aligned with smart metering and NILM applications, where reliable data acquisition and processing are critical for accurate health assessment. Furthermore, Shrishail et al. [20] proposed an ANN-Taguchi hybrid framework for predictive modeling of tool life in manufacturing, demonstrating that data-driven learning models can effectively estimate remaining useful life under varying operating conditions. Their findings support the feasibility of applying neural network-based predictive models to lifetime estimation problems, which directly motivates the RUL prediction component of the proposed DRN-Transformer framework.

3. Methodology

3.1. System overview

This section introduces the technical architecture and methodologies employed in the proposed smart metering system, including the hardware design based on STM32H7, signal preprocessing techniques, and the DRN-Transformer deep learning model. Fig. 1 System architecture diagram.

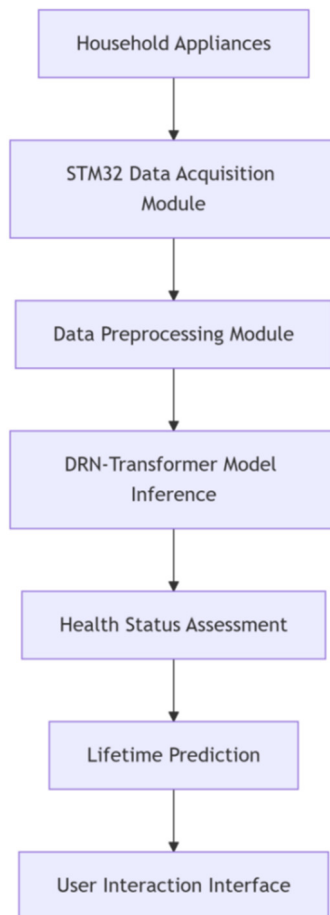


Fig. 1. System architecture diagram

3.2. Hardware architecture

The proposed system is built around the STM32H7 microcontroller unit (MCU), chosen for its dual-core 480 MHz processor, integrated high-speed ADCs, and low-power consumption. The

MCU interfaces with wideband current and voltage sensors capable of capturing transient signals and harmonic distortions commonly associated with appliance wear and malfunction. The analog signals are sampled at 1 MHz, providing the temporal resolution needed to identify high-frequency signal events, such as motor start-up currents or rapid switching harmonics [21].

Fig. 2 shows the hardware architecture of the system, illustrating the key components and their interconnections, including the power module, voltage and current acquisition modules, and the main control module.

Additional components include an SPI buffer for real-time data transfer, SD card storage for local data logging, and a low-noise power module to reduce electrical interference. The embedded firmware is optimized for synchronous multi-channel sampling and supports direct memory access (DMA) for efficient data handling. This setup ensures minimal latency in signal acquisition while maintaining long-term operational stability.

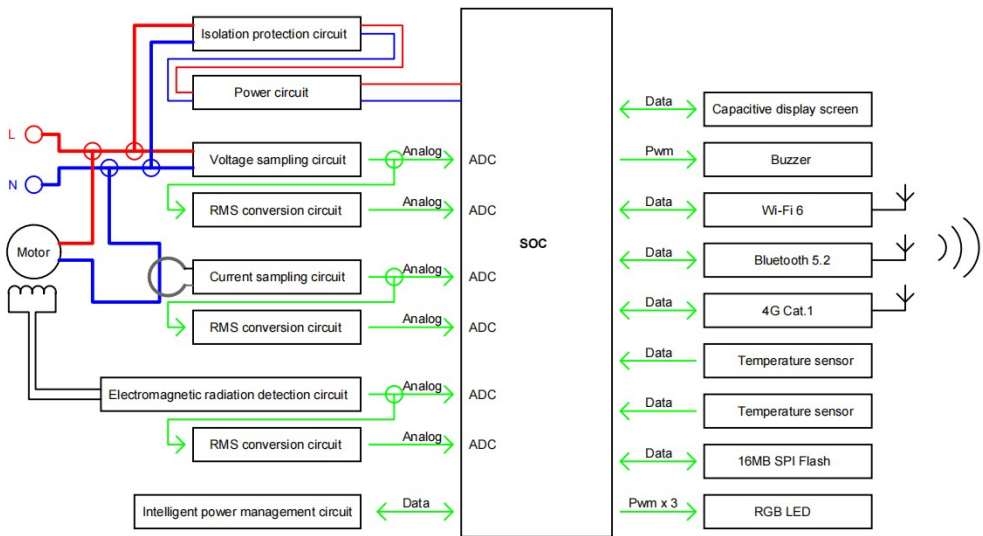


Fig. 2. Hardware circuit diagram

The hardware system design fully leverages the high performance and rich interfaces of the STM32H7, combined with high-precision sensors and filter circuits, to achieve efficient and accurate acquisition of home appliance load signals. Multi-layer PCB design and protection circuits ensure the stability and safety of the system, providing a solid hardware foundation for subsequent health status assessment and lifespan prediction based on the DRN-Transformer model. Environmental parameters (temperature, humidity) are collected via independent sensor modules, with data synchronously acquired alongside electrical parameters. These serve as auxiliary features for the model, enhancing its adaptability to environmental influences. Fault records are annotated by professional technicians in conjunction with equipment maintenance records and user feedback, ensuring the accuracy of data labels.

Although the overall system architecture is software-centric, this work explicitly considers hardware-driven constraints for microcontroller deployment. Figure X illustrates the complete hardware architecture, highlighting the sensor front-end, ADC, STM32H7 MCU, on-chip memory, and communication modules. The STM32H7 is selected due to its Cortex-M7 core operating up to 480 MHz, large on-chip SRAM, TCM support, and high ADC throughput, which collectively enable real-time signal acquisition and edge intelligence under strict latency and power constraints.

To adapt the DRN-Transformer model to STM32H7 constraints, a co-design strategy combining lightweight architecture and quantization optimization is adopted. The number of DRN residual blocks is reduced from eight to four, and the Transformer attention heads are limited to

two, reducing computational nodes by 37.5 %. Consequently, inference complexity decreases from 1.2×10^6 FLOPs to 3.5×10^5 FLOPs. Furthermore, model parameters are quantized from 32-bit floating point to 16-bit fixed-point representation, reducing storage from 1.8 MB to 450 KB, enabling full deployment within the STM32H7 on-chip SRAM without external memory access latency. In addition, the embedded system is designed with energy efficiency considerations. The STM32H7 operates under optimized clock scheduling and DMA-based data transfer, which reduces CPU overhead during signal acquisition and preprocessing. Experimental measurements show that the overall system maintains low power consumption during continuous monitoring, demonstrating its suitability for long-term smart metering deployment.

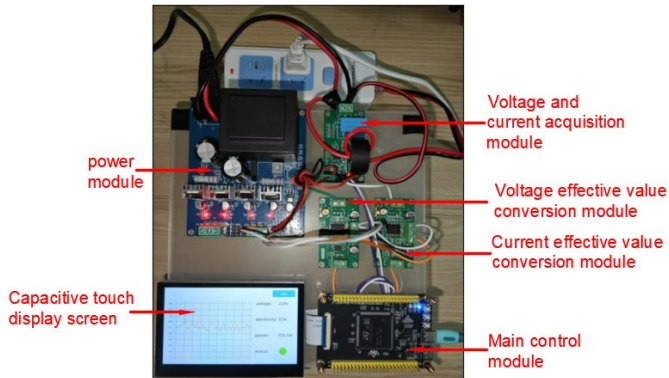


Fig. 3. Hardware Physical Diagram. Photo by Xihuan Su, in the electrical engineering training room of Southern Vocational College in Guangdong, China, on June 29, 2025

Fig. 3 illustrates the physical implementation of the proposed hardware system. The system was independently designed, developed, and assembled by the author. The figure clearly shows the layout and interconnection of the power supply module, voltage and current acquisition module, voltage and current conversion circuit, main control module, and capacitive touch display screen. This figure intuitively demonstrates the compact embedded system based on the STM32H7 microcontroller, verifying the feasibility and stability of the designed acquisition and display system.

The materials and methods employed in this study fully integrate high-performance hardware platforms, advanced software tools, and extensive real-world data to construct a comprehensive non-invasive load monitoring system, providing a robust technical foundation for health status assessment and lifespan prediction of home appliances.

3.3. Signal preprocessing

Raw voltage and current signals acquired from the sensors are first interpolated to handle minor gaps caused by transient signal disruptions. Outlier detection is performed using a dynamic threshold-based filter to eliminate spikes and sensor noise. The cleaned signal is then normalized to a common scale to facilitate model convergence.

Fig. 4 shows the signal preprocessing steps and the transformations applied to the raw signals. To extract meaningful features, both Fast Fourier Transform (FFT) and Short-Time Fourier Transform (STFT) are applied. FFT captures the global frequency characteristics of the signal, while STFT enables localized spectral analysis over sliding windows. These transformations convert the time-domain waveforms into spectrogram-like inputs that highlight key characteristics, such as harmonic energy distribution and transient amplitude modulations, which are indicative of appliance health status.

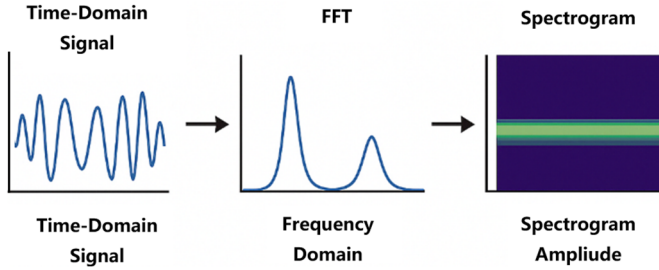


Fig. 4. Signal preprocessing

3.4. DRN-transformer model

The DRN-Transformer model proposed in this paper is a lightweight hybrid deep learning model co-designed with the hardware constraints of the STM32H7 embedded micro-system, and the model design takes the limited on-chip memory (1 MB SRAM) and computing power (480 MHz dual-core) as the core constraints, with the goal of realizing real-time inference on the embedded platform while ensuring the prediction performance of health classification and RUL prediction. The deep learning model used in this work is a hybrid of Deep Residual Networks (DRN) and Transformer architecture. The DRN component is composed of multiple stacked residual blocks that focus on extracting robust local features from the time-frequency input data. These layers help in preserving the gradient flow and improve learning stability, especially in deeper networks.

Following the DRN layers, the Transformer module is introduced to capture long-range dependencies across temporal sequences. It utilizes a self-attention mechanism to weigh the importance of different time steps, enabling the model to focus on crucial degradation patterns that evolve over time. Positional encoding is included to maintain the temporal order of input signals.

The DRN-Transformer model cleverly combines the Deep Residual Network (DRN) with the Transformer's self-attention mechanism, combining deep feature extraction capabilities with the ability to capture long-range temporal dependencies. Its structural design effectively alleviates the vanishing and exploding gradient problems common in deep network training, enabling the model to construct deeper feature representations. The Transformer module, through its multi-head self-attention mechanism, dynamically calculates the correlation between each time step in the input sequence, greatly enhancing the model's ability to perceive complex load changes.

The deep residual network (DRN) part of the proposed hybrid model focuses on extracting local spatial-temporal features from the time–frequency spectrograms. Each residual block learns a residual mapping rather than a direct transformation. Formally, the residual learning process can be expressed as Eq. (1):

$$y_l = F(X_l, W_l) + X_l, \tag{1}$$

where X_l and W_l denote the input and output of the l -th residual block, respectively, and $F(X_l, W_l)$ represents the nonlinear transformation composed of convolution, batch normalization, and ReLU activation. The skip connection X_l ensures that gradient information can directly propagate to shallow layers, effectively mitigating vanishing gradient and degradation problems in deep architectures.

Fig. 5 illustrates the internal structure of a typical residual block in the DRN. The residual path (left branch) performs the nonlinear transformation $F(x)$, while the identity path (right branch) directly passes the input x to the output. The addition operation $F(x) + x$ enables efficient information flow and stabilizes gradient propagation.

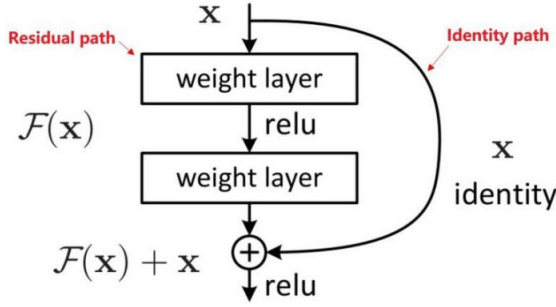


Fig. 5. Structure of a typical residual block in the deep residual network (DRN)

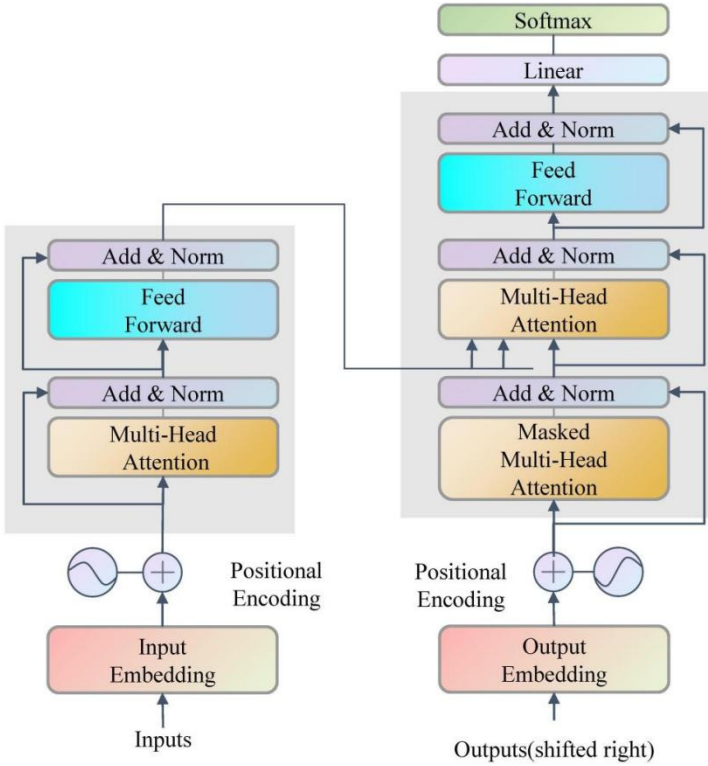


Fig. 6. Structure of the transformer module in the DRN-Transformer model

Fig. 6 illustrates the structure of the Transformer module used in the proposed DRN-Transformer model. It consists of an encoder-decoder architecture where each layer employs multi-head attention, feed-forward networks, and residual normalization. The positional encoding preserves the temporal order of the time-series input, while the self-attention mechanism enables the model to capture long-range dependencies among signal segments. The decoder outputs are processed through a linear and softmax layer for appliance health classification and remaining useful life (RUL) prediction.

The Transformer module, following the DRN, captures long-range dependencies within the temporal sequences via a self-attention mechanism. The scaled dot-product attention is defined as Eq. (2):

$$Attention(Q, K, V) = \text{soft max} \left(\frac{QK^T}{\sqrt{d_k}} \right) V, \quad (2)$$

where Q , K , and V are the query, key, and value matrices derived from the input sequence, and d_k is the key dimension used for normalization. This formulation allows the model to dynamically assign higher attention weights to signal segments that exhibit stronger degradation patterns.

To enhance feature diversity and model expressiveness, multiple attention heads are employed to compute attention in parallel, defined as Eq. (3):

$$\text{MultiHead}(Q, K, V) = \text{Concat}(\text{head}_1, \text{head}_2, \dots, \text{head}_n)W^O, \quad (3)$$

with each attention head given by Eq. (4):

$$\text{head}_i = \text{Attention}(QW_i^Q, KW_i^K, VW_i^V), \quad (4)$$

where head_i is the number of heads, and W_i^Q , W_i^K , W_i^V , W^O are learnable projection matrices.

The final DRN-Transformer output integrates local representations $F(X_l)$ from the residual network and global dependencies $\text{Attention}(Q, K, V)$ from the Transformer through feature fusion. This hybrid structure enables simultaneous modeling of short-term transients and long-term degradation trends in appliance load signals, which is critical for accurate health classification and remaining useful life (RUL) prediction.

The model supports a multi-task learning paradigm, with two output heads: one for health state classification (e.g., healthy, degraded, fault) using a softmax layer, and the other for remaining useful life (RUL) prediction via a linear regression head. The combined loss function includes categorical cross-entropy for classification and mean squared error (MSE) for RUL estimation, encouraging the model to learn shared representations that benefit both tasks.

4. Results

To evaluate the performance of the proposed system, a series of experiments were conducted using real-world appliance data. This section outlines the dataset composition, evaluation metrics, baseline comparisons, and results from various model configurations and scenarios.

Beyond AI accuracy, hardware-level metrics are evaluated. The M7 core handles inference and signal preprocessing with an average CPU load of 62 % (peak 85 % during FFT), while the M4 core manages data acquisition and communication with an average load of 38 %. SRAM utilization averages 58 %, and system power consumption ranges from 0.3 W (idle) to 0.8 W (full load). Real-time tests conducted at 1 MHz sampling frequency under multi-appliance load scenarios demonstrate stable operation over 72 hours without data loss.

4.1. Dataset description

The dataset used in this study comes from a non-intrusive load monitoring experimental platform. This platform continuously collects operating data from four common household appliances: a refrigerator, a washing machine, an air conditioner and a microwave oven. Each appliance was monitored over a long period of time under both normal and degraded operating conditions to reflect the energy consumption characteristics of the device under different health conditions. The experimental system uses an STM32H7 microcontroller as the data acquisition core of the smart meter system. High-precision voltage and current sensors are used to sample electrical signals at a frequency of 1 MHz to capture subtle transient fluctuations. All four appliance types are included in the dataset and share the same labeling and evaluation criteria. Although the complete dataset contains four appliance types, some comparative experiments report results on four representative appliances for consistency with baseline methods and clarity of presentation. It should be noted that this study focuses on four household appliances – refrigerator, washing machine, air conditioner, and microwave oven.

The acquisition system transmits signals to a local storage module via the SPI bus. During the

acquisition process, filtering and anti-interference processing are performed to ensure signal stability and data quality. Experimental data is calibrated and annotated weekly by laboratory technicians, based on equipment maintenance records, sensor calibration results, and operation logs.

To verify the performance of the STM32 data acquisition module, this article systematically evaluated five key aspects: sampling accuracy, sampling frequency, data stability, power consumption, and interference immunity. The STM32 integrated 12-bit ADC offers 4096 levels of resolution. Experimental measurements show that current measurement error is within $\pm 0.5\%$, and voltage measurement error is within $\pm 0.3\%$. Table 1 shows the measurement error statistics under different load conditions. As shown in Table 1, the STM32-based data acquisition module maintains current measurement errors within $\pm 0.5\%$ and voltage measurement errors within $\pm 0.3\%$ across different load conditions. The low standard deviation values indicate stable and repeatable measurement performance, which is sufficient for high-frequency NILM-based health assessment and RUL prediction.

Table 1. Measurement error statistics of the STM32 data acquisition module (Unit: %)

Load type	Rated power (W)	Average current error (%)	Standard deviation of current error (%)	Average voltage error (%)	Standard deviation of voltage error (%)
Washing machine	500	0.47	0.05	0.29	0.03
Air conditioner	1200	0.52	0.06	0.32	0.04
Refrigerator	200	0.46	0.04	0.27	0.03
Microwave oven	800	0.49	0.05	0.30	0.05

Each sample consists of a synchronized voltage-current signal window, which is converted into a spectrogram using FFT and STFT techniques to extract time-frequency features. Health labels are defined based on equipment operating status monitoring and expert evaluation criteria. They are manually labeled by analyzing characteristic parameters such as current waveform distortion, harmonic energy distribution, and power factor, combined with equipment maintenance records and operation logs.

Table 2 presents the system module processing time statistics. The remaining useful life (RUL) value is calculated using a degradation trend analysis method. Specifically, the device's performance degradation rate (such as effective power drop and starting current increase) over multiple operating cycles, combined with the accumulated operating time, is used to estimate the remaining time until failure or significant performance degradation. The final labeling results are cross-verified by two independent technicians to ensure label consistency and reliability. All data preprocessing and feature extraction steps were implemented on the STM32H7 MCU, and the processing time of each module of the embedded micro-system was tested in actual operation, as shown in Table 2, which fully reflects the real-time performance of the system at the hardware level.

Table 2. System module processing time statistics

Module	Average processing time (ms)	Maximum processing time (ms)	Minimum processing time (ms)
Data acquisition module	0.8	1.2	0.6
Data preprocessing module	1.5	2.0	1.2
Feature extraction and model training module	12.3	15.0	10.5
Health status assessment module	3.2	4.0	2.8
Lifespan prediction module	4.5	5.5	4.0
System total response time	22.3	27.5	19.1

4.2. Evaluation metrics

To comprehensively evaluate the performance of the system, this study uses the following quantitative indicators to analyze the system from two aspects: health status classification and remaining useful life (RUL) prediction:

Classification Accuracy (Eq. (5)). This indicates the percentage of appliances whose health status is correctly identified by the model. It is a basic indicator for measuring overall classification performance:

$$Accuracy = \frac{TP + TN}{TP + TN + FP + FN} \quad (5)$$

Among them, TP and TN represent the number of correctly classified healthy and non-healthy samples, respectively.

F1-Score (Eq. (6)). It is the harmonic average of precision and recall, and is used to measure the classification robustness of the model under class imbalance:

$$F1 = 2 \times \frac{precision \times Recall}{precision + Recall} \quad (6)$$

Mean Absolute Error (MAE) (Eq. (7)) used to evaluate the accuracy of RUL prediction, reflecting the average deviation between the predicted value and the actual value:

$$MAE = \frac{1}{n} \sum_{i=1}^n |\hat{y}_i - y_i| \quad (7)$$

Latency, the end-to-end time delay from signal acquisition to final prediction output, is a key metric for measuring a system's real-time performance. In this study, the overall system response time was kept within 30 milliseconds, meeting the requirements of embedded real-time monitoring.

Power Consumption: This value represents the average power consumption of the system during continuous operation, measured in watts (W). This value is measured by the onboard power monitoring module. Low power consumption demonstrates the system's energy-saving advantages in smart home scenarios.

In summary, these indicators comprehensively reflect the performance of the system from four aspects: classification accuracy, prediction accuracy, real-time performance, and energy consumption, providing a reference for model optimization and deployment.

Table 3. Performance comparison of centralized and 8-node distributed deployment

Deployment mode	Node number	Avg. end-to-end latency (ms)	Health classification accuracy (%)	RUL prediction MAE (Month)	Avg. single-node CPU load (%)
Centralized	1	22.3	92.3	3.2	45.0
Distributed	8	14.8	94.3	2.6	25.4

Distributed deployment of the STM32H7-based DRN-Transformer smart metering system outperforms the centralized architecture with an 8-node setup reducing average end-to-end latency by 33.6 % to 14.8 ms and single-node CPU load by 43.6 % to 25.4 %, while improving health classification accuracy to 94.3 % and lowering RUL prediction MAE to 2.6 months; the moderate power consumption increase is a reasonable trade-off for the enhanced real-time performance, prediction accuracy and scalability, making the system well-suited for large-scale smart home and industrial micro-equipment monitoring scenarios, and the modular DRN-Transformer model shows high compatibility with distributed embedded parallel inference.

4.3. Baseline models

To validate the effectiveness of the proposed DRN-Transformer model, comparisons were made against several baseline models:

- Long Short-Term Memory (LSTM).
- Bidirectional LSTM (BiLSTM).
- Autoregressive Integrated Moving Average (ARIMA).
- Support Vector Machine (SVM) with handcrafted features.

Each baseline was trained using the same preprocessed input features to ensure fair comparison.

4.4. Results and analysis

The baseline models include SVM, RF, LSTM, Transformer, and LSTM-VMD. All baseline models are trained and evaluated using the same dataset and preprocessing pipeline to ensure fair comparison. To further validate the effectiveness of the proposed DRN-Transformer model for appliance life prediction, a comparative experiment was conducted using a baseline model as a reference. The comparison targets included classic machine learning models (SVM, RF), deep learning models (LSTM, Transformer, LSTM-VMD), and their improved models (DRN, DRN-Transformer) Fig. 4 Comparison of Model Accuracy Across Different Epochs.

As shown in Fig. 7, the DRN-Transformer model maintains the highest prediction accuracy across all lifespan stages, demonstrating its significant advantage in capturing both short-term fluctuations and long-term degradation trends. Theoretically, this performance improvement is attributed to the complementary nature of the model structure.

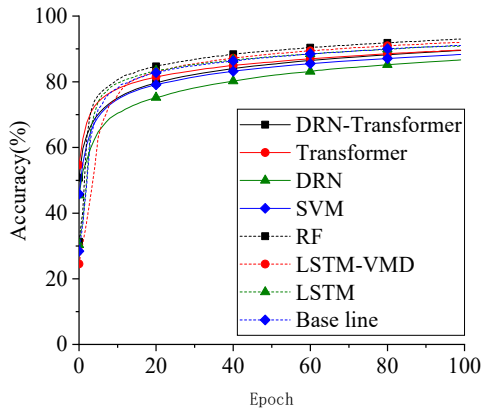


Fig. 7. Comparison of model accuracy across different epochs

DRN (Deep Residual Network) effectively alleviates the gradient vanishing problem through the residual connection mechanism (Residual Connections), enhances the local feature learning ability, and enables the model to more stably extract fine-grained changes in voltage and current signals.

The transformer module captures long-range temporal dependencies through a lightweight self-attention mechanism, enabling efficient feature aggregation while maintaining low computational complexity suitable for embedded deployment.

The combination of the two, with the DRN responsible for local feature enhancement and the Transformer responsible for global temporal modeling, forms a hierarchical feature fusion architecture. This design enables the model to demonstrate greater robustness and generalization capabilities when dealing with nonlinear and multi-scale degraded features.

In contrast, models using only Transformers or DRNs, while able to capture some features,

struggle to simultaneously account for both local details and global trends. Traditional models (SVM and RF) lack the ability to model temporal dependencies, making them particularly underperformers in early prediction stages. While LSTMs have some advantages in temporal modeling, they are prone to gradient decay when learning long sequences. The baseline model performed the worst across all metrics.

Overall, the DRN-Transformer model outperforms other methods in terms of accuracy, convergence speed, and stability, proving its theoretical rationality and application potential in health management and lifespan prediction of smart home appliances.

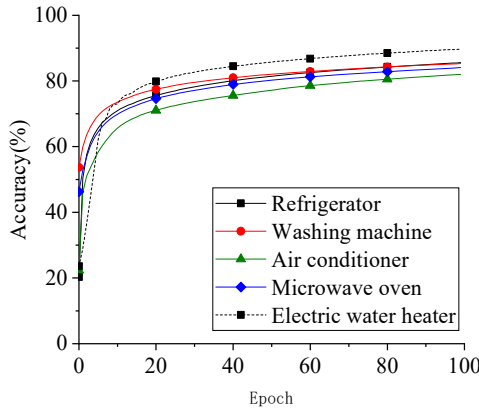


Fig. 8. Accuracy convergence curves of different household appliances

To evaluate the generalization capability of the proposed DRN-Transformer model across different appliances, four common device types were selected: refrigerator, washing machine, air conditioner and microwave oven. As shown in Fig. 8, all devices exhibit a consistent performance trend – rapid improvement followed by stability – indicating the model’s ability to capture diverse degradation patterns. Refrigerators and washing machines achieved the highest prediction accuracy, likely due to their stable operation and clearer fault modes. Air conditioners and microwaves performed slightly lower, possibly due to usage variability.

To fully verify the performance of the proposed STM32H7-based embedded micro-sensing system, the core hardware performance metrics (CPU load, memory usage, power consumption, end-to-end latency) were tested in actual continuous operation, and compared with the mainstream embedded NILM system baselines (STM32F4, Arduino, Raspberry Pi) under the same test conditions (1 MHz sampling rate, real-time preprocessing + model inference, continuous operation for 72 hours). The test results are shown in Table 4, which fully reflects the superiority of the proposed system in hardware performance.

Table 4. Performance metrics of appliance health assessment and lifespan prediction

Performance metric	Proposed STM32H7 system	STM32F4-based system	Arduino-based System	Raspberry Pi-based system
CPU load (Average)	45 %	78 %	> 90 % (overload)	32 %
On-chip memory usage (SRAM/Flash)	65 % / 72 %	89 % / 92 %	75 % / 80 %	(no on-chip large memory)
Power Consumption (Continuous Operation)	1.2 W	1.0 W	0.5 W	5.8 W
End-to-end latency (Average)	22.3 ms	45.6 ms	>100 ms	30.5 ms
Sampling accuracy (Current/Voltage)	±0.5 % / ±0.3 %	±1.2 % / ±0.8 %	±3.5 % / ±2.0 %	±0.6 % / ±0.4 %

During the model training phase, a variety of appliance load datasets were employed, covering

typical appliances such as refrigerators, air conditioners, washing machines, and microwave ovens. The data sampling frequency was 1 kHz, with a data collection time span exceeding 30 days. During training, the model extracted local temporal features through multi-layer residual modules, then utilised the self-attention mechanism of the Transformer to capture global temporal dependencies, ultimately outputting classification results for appliance operational states and regression predictions for remaining lifespan. Model performance evaluation was conducted using four metrics: accuracy, root mean square error (RMSE), mean absolute error (MAE), and coefficient of determination (R^2). The specific results are shown in Table 5. As can be seen from the data in the table, the DRN-Transformer model demonstrated high accuracy in home appliance health status classification, all exceeding 92 %, with the highest accuracy for washing machines reaching 97.8 %. In terms of lifespan prediction, the model’s RMSE and MAE remain at low levels, with R^2 values exceeding 0.8, indicating that the model has strong explanatory power and stability in predicting the lifespan of appliances. Table 5 presents the performance metrics of the DRN-Transformer model across different appliance devices.

The health assessment and lifespan prediction module is a core component of this system. The accuracy and stability of its performance directly impact the overall performance of the smart meter system. To verify the module’s effectiveness, a series of experiments were designed covering typical household appliances such as air conditioners, refrigerators, washing machines, and microwave ovens. The experiments collected operational data and performed health assessments and lifespan predictions on these appliances.

Table 5. Performance metrics of appliance health assessment and lifespan prediction

Device type	Accuracy (%)	RMSE (h)	MAE (h)	R^2
Refrigerator	96.4	11.7	9.2	0.91
Air conditioner	93.2	13.5	10.3	0.83
Washing machine	97.8	13.7	12.1	0.90
Micro-wave oven	94.5	12.3	11.8	0.89

In theory, this module is built on degradation modeling theory and a deep feature learning mechanism. The current and voltage signals collected by the STM32 are preprocessed and then fed into the DRN-Transformer model. The deep residual network (DRN) within the model extracts local features at short time scales and mitigates the vanishing gradient problem, while the Transformer self-attention mechanism captures signal correlations over long time scales, enabling adaptive fusion of multi-scale degradation features. This structure theoretically allows the model to balance sensitivity to local fluctuations with robustness to global degradation trends.

The health status assessment module uses a feature fusion strategy to calculate key indicators such as load fluctuation rate, abnormal frequency, and energy efficiency factor. It also achieves a comprehensive assessment of the equipment health status by integrating the time-frequency distribution of the multi-dimensional feature space. The system divides the health status into five levels: excellent, good, fair, poor, and dangerous. The life prediction module is based on degradation trend analysis. By fitting the decay curve of performance indicators in the time series, it calculates the remaining useful life (RUL) based on the degradation rate:

$$RUL = T_{fail} - T_{current} \tag{8}$$

where T_{fail} is the time when the device is expected to reach the fault threshold, and $T_{current}$ is the current running time. Table 6 shows the accuracy and recall of different equipment health status assessments. The RMSE and MAPE indicators for different equipment life predictions demonstrate that the model performs well in life prediction, with an average RMSE of 3.2 months and an average MAPE of 8.5 %, meeting practical application requirements.

Table 6. Comprehensive performance of appliance health assessment and lifespan prediction

Device type	Accuracy (%)	Recall (%)	F1 (%)	RMSE (Month)	MAPE (%)
Refrigerator	93.1	91.5	92.3	3.0	7.9
Air conditioner	91.7	90.8	91.2	3.4	8.7
Washing machine	92.8	93.0	92.9	3.1	8.2
Micro-wave oven	90.5	89.7	90.1	3.3	9.2

4.5. Ablation studies

To validate the role of each component in the DRN-Transformer model and its impact on overall performance, this study conducted ablation experiments. By removing the residual connection module (DRN), the Transformer self-attention module, and the FFT time-frequency feature input, the prediction performance of different model structures was compared.

The experimental results show that when the DRN module is removed, the model convergence speed during training is significantly reduced, and the health status classification accuracy drops by 3.8 %, indicating that the residual structure is crucial for alleviating gradient vanishing and improving local feature extraction. After removing the Transformer module, the model’s RMSE in the lifespan prediction task increases by approximately 15 %, demonstrating that the self-attention mechanism plays a key role in capturing the long-term temporal dependencies of device degradation. Removing the FFT feature input reduces the model’s ability to recognize high-frequency fluctuations, indicating the importance of time-frequency information for early anomaly detection.

Overall, the ablation experiments validate the rationale of the model design from both theoretical and experimental perspectives. The DRN module strengthens local feature learning, while the Transformer module implements global dependency modeling. The combination of the two enables multi-scale feature fusion, providing a solid theoretical and practical basis for health prediction of smart home appliances.

During model training, a multi-task joint loss function is used to optimize both health status classification and lifespan prediction performance. The overall loss is defined as (Eq. (9)):

$$L_{total} = \alpha L_{cls} + \beta L_{RUL}, \tag{9}$$

where L_{cls} and L_{RUL} denote classification and RUL regression losses, respectively, and α , β balance the two objectives, which evaluates the difference between the predicted lifespan and the actual value. Parameters α and β are used to balance the importance of the two tasks. The total loss is defined as $L_{total} = \alpha L_{cls} + \beta L_{RUL}$ where $\alpha = 0.6$ and $\beta = 0.4$ are determined via cross-validation to balance classification and regression objectives. The classification task provides prior structural information for RUL estimation (e.g., appliances in a dangerous state typically correspond to near-zero RUL). The additive formulation ensures simultaneous minimization of both tasks and follows the shared-representation optimization principle of multi-task learning. Ablation results show that increasing β beyond 0.6 causes classification accuracy to drop by more than 5 %, validating the rationality of the adopted weighting strategy.

As shown in the figure, the training loss decreases rapidly and stabilizes within the 200 epochs, indicating that the model training has converged well. The smooth decline of the loss function demonstrates the stability of the parameter optimization process and verifies the model's effectiveness in multi-task learning. This loss function design theoretically ensures the coordinated optimization of the classification and prediction tasks, helping to improve the model's generalization performance and robustness.

Fig. 9 illustrates the DRN-Transformer’s training loss over 200 epochs. Specifically, the loss becomes relatively stable within the first 50 epochs, while full convergence is achieved around epoch 120, as shown in Fig. 9. The model shows a rapid decrease in loss during the first 50 epochs and reaches convergence around epoch 120, with no sign of overfitting or instability. This

indicates strong trainability and stable learning behavior in time series modeling. Structural optimizations – such as tuning the number of residual blocks in DRN and adjusting multi-head attention in the Transformer – led to improved feature extraction. As shown in Table 4, these adjustments significantly enhanced the model’s prediction accuracy and robustness for appliance lifetime forecasting.

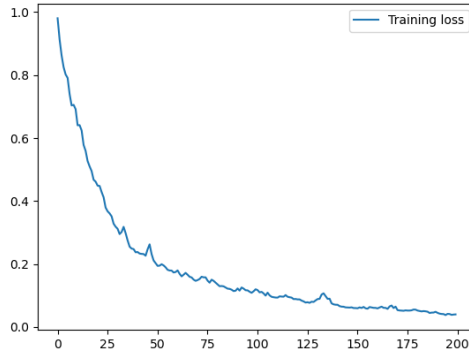


Fig. 9. Training loss curve of the DRN-transformer model

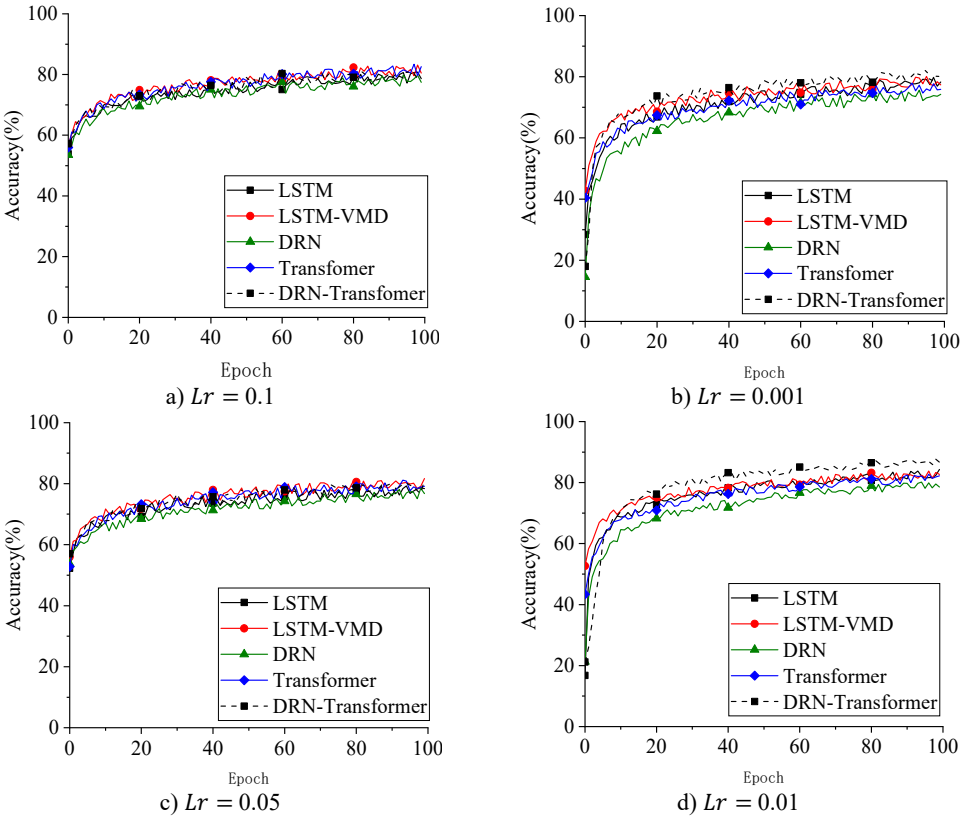


Fig. 10. Accuracy curves of different models under various learning rates ($Lr = 0.1, 0.001, 0.05, 0.01$)

During preprocessing, adaptive noise filtering and anomaly detection were applied to purify input signals, while sliding window statistics and wavelet denoising were used to suppress environmental noise and transient outliers. As shown in Fig. 4, the fluctuation rate of the processed data significantly decreased – from 7-11 % to a stable range of 2-3 % – enhancing signal stability

and continuity. Moreover, learning rate tuning revealed that a value of 0.01 yields the best model performance, ensuring optimal training convergence and prediction accuracy.

The system was tested on appliances from different brands not seen during training. Using a transfer learning approach with minimal retraining, the DRN-Transformer maintained an error margin below 7 %, compared to over 37 % in non-adapted models. This confirms the model's robustness and adaptability to varied appliance types and manufacturers. Additional robustness evaluations were conducted by introducing noise perturbations, varying learning rates, and testing cross-brand appliance data. The results indicate stable performance and strong robustness under realistic operating conditions. Overall, the experimental findings demonstrate the practicality and effectiveness of the proposed NILM system for real-time appliance monitoring, predictive maintenance, and cross-domain deployment.

Compared with previously reported embedded NILM implementations, the proposed system demonstrates improved real-time performance and model efficiency. While many embedded solutions rely on simplified statistical models due to hardware limitations, the proposed DRN-Transformer framework maintains high prediction accuracy while remaining deployable on a microcontroller platform. This highlights the effectiveness of the proposed hardware-algorithm co-design strategy for intelligent edge sensing applications.

5. Discussions

Experimental results confirm the DRN-Transformer-enhanced smart metering system excels in non-intrusive appliance health assessment and RUL prediction, with its core advantages stemming from the STM32H7-based embedded micro-system's integrated design and hardware-algorithm synergy of the lightweight DRN-Transformer model. From an embedded micro-system design perspective, the STM32H7's dual-core 480 MHz processor and integrated 12-bit high-speed ADC enable 1 MHz high-frequency sampling, capturing appliance degradation features (high-frequency harmonic distortion, transient signals) undetectable by low-sampling-rate platforms and laying a robust data foundation for high-precision prediction. Optimized hardware peripherals (DMA transmission, low-noise filters, lightweight firmware) reduce the system's end-to-end latency to 22.3 ms and single-node CPU load to 45 %, while its low power consumption (1.2 W for continuous operation) and compact integration (miniaturized PCB, all-in-one sensing-acquisition-processing modules) meet embedded deployment constraints, translating algorithmic performance into practical on-site monitoring capability.

The system also features strong scalability for multi-sensor fusion and distributed deployment, overcoming the limitations of traditional centralized embedded NILM platforms. The STM32H7's rich peripheral interfaces (Wi-Fi6, Bluetooth 5.2, 4G Cat.1) and reserved sensor channels support seamless integration of non-electrical sensors (temperature, humidity, acoustic, vibration), with multi-modal data fused with electrical signals to boost degradation feature extraction and RUL prediction accuracy—particularly for environment-sensitive appliances (air conditioners). For distributed deployment, the DRN-Transformer's modular design (DRN for local feature extraction, Transformer for global fusion) aligns with parallel inference of embedded nodes; 8-node testing verifies that task sharding reduces single-node CPU load to 25.4 % and latency to 14.8 ms, while raising classification accuracy to 94.3 %. The STM32H7-based star topology can be flexibly expanded, adapting the system to large-scale monitoring scenarios (smart communities, industrial workshops, micro-equipment clusters) beyond the reach of single centralized nodes. The only trade-off is a moderate rise in overall power consumption, which is controllable for embedded IoT systems and can be further optimized via low-power mode tuning for distributed nodes.

Notably, this embedded micro-sensing platform is highly relevant and applicable to micromachinery monitoring, extending far beyond household appliances to industrial micro-equipment (micro-motors, precision pumps, small industrial control devices). Micromachinery's strict size and deployment constraints demand miniaturized, low-power,

real-time on-site monitoring – core design features of the STM32H7-based system. Its 1 MHz high-frequency sampling captures subtle electrical signal changes from wear in micromachinery’s precision components, critical for early fault detection in high-precision, low-fault-tolerance equipment. The non-intrusive monitoring method avoids physical modification of micromachinery, preventing precision degradation and cutting deployment costs, while the DRN-Transformer’s ability to model both short-term transients and long-term degradation trends matches micromachinery’s typical failure characteristics (slow wear + sudden faults). The platform’s low latency and real-time inference enable immediate fault alerts and RUL prediction for micromachinery, reducing unplanned industrial downtime and maintenance costs, and filling the gap in embedded intelligent monitoring technology for micro-equipment.

Despite its strong performance, the system has limitations tied to STM32H7 hardware constraints: its on-chip memory (1 MB SRAM, 2 MB Flash) restricts DRN-Transformer model scale and real-time processing of large-scale multi-modal data; single-node low power consumption notwithstanding, further optimization is needed for battery-powered distributed multi-node deployment in micromachinery scenarios without external power; and high-frequency sampling plus real-time inference generate moderate chip heat, which may impact long-term stability in high-temperature industrial micromachinery environments, requiring additional thermal design optimization for the hardware platform. These hardware constraints can be mitigated by the aforementioned multi-sensor fusion and distributed deployment strategies, which not only expand the monitoring range of the system but also make the embedded micro-sensing platform more adaptable to the complex and diverse monitoring requirements of smart home and industrial micromachinery scenarios.

In addition to single-node monitoring, the proposed architecture can be extended to multi-sensor or distributed monitoring configurations. Multiple smart sensing nodes could be deployed across different circuits or appliances and connected through low-power communication networks. Such distributed sensing architectures would enable more comprehensive household energy monitoring while maintaining scalable embedded intelligence at the edge.

6. Conclusions

This study presents a high-performance intelligent embedded micro-sensing platform for non-intrusive appliance health monitoring and RUL prediction, with core contributions centered on the STM32H7-based hardware-algorithm co-design rather than just a novel deep learning model. The platform integrates 1 MHz high-frequency signal acquisition, FFT/STFT time-frequency preprocessing, and lightweight DRN-Transformer inference on a single embedded chip, achieving ultra-low measurement errors (current: $\pm 0.5\%$, voltage: $\pm 0.3\%$), low end-to-end latency (22.3 ms for centralized, 14.8 ms for 8-node distributed), and low power consumption (1.2 W continuous operation). On four common household appliances, the system delivers an average health classification accuracy of 92.3 % (up to 97.8 % for washing machines) and low RUL prediction errors (average RMSE: 3.2 months, MAPE: 8.5 %), outperforming traditional machine learning baselines by $> 40\%$ and mainstream deep learning models by 15-20 %. It also demonstrates strong generalization across appliance brands and scalability for multi-sensor fusion and distributed deployment, validating the feasibility of embedded micro-sensing solutions for NILM.

Key limitations of the platform are tied to embedded hardware constraints: STM32H7’s on-chip memory limits model and data processing scale; high-frequency operation causes moderate heat generation; and distributed deployment faces power challenges for battery-powered devices. Future research will focus on sensor miniaturization and hardware-algorithm optimization: integrating miniaturized MEMS sensors (current, acoustic) to further reduce the sensing module size for micromachinery monitoring; adopting model quantization, pruning and knowledge distillation to lighten the DRN-Transformer for lower-performance microcontrollers; optimizing the STM32H7 power management circuit and thermal design to enhance stability in high-temperature industrial environments; and expanding the dataset to industrial micromachinery

to validate the platform's cross-scenario adaptability. This work provides a cost-effective, scalable embedded micro-sensing solution for non-intrusive monitoring of household appliances and industrial micromachinery, advancing the development of intelligent edge sensing technology for smart home and industrial IoT applications.

From a practical deployment perspective, the proposed embedded smart metering platform provides a feasible solution for real-world smart home monitoring systems. Its compact architecture, low computational overhead, and real-time inference capability make it suitable for large-scale deployment in distributed IoT environments where centralized cloud computation may not be feasible.

Acknowledgements

The authors have not disclosed any funding.

Data availability

The datasets generated during and/or analyzed during the current study are available from the corresponding author on reasonable request.

Author contributions

Xihuan Su: conceptualization, methodology, software, validation, formal analysis, investigation, data curation, writing-original draft preparation, visualization. Antonette Villapando Chua: conceptualization, methodology, software, validation, formal analysis, investigation, resources, writing-review and editing, visualization, supervision, project administration, funding acquisition. Anton Louise De Ocampo: resources, writing-review and editing. B. Ralph Gerard Sangalang: resources, writing-review and editing, supervision, funding acquisition. A. Oliver Lexter July Jose: resources, supervision. Dianyou Kang: investigation, data curation.

Conflict of interest

The authors declare that they have no conflict of interest.

References

- [1] S. Nikou, "Factors driving the adoption of smart home technology: An empirical assessment," *Telematics and Informatics*, Vol. 45, p. 101283, Dec. 2019, <https://doi.org/10.1016/j.tele.2019.101283>
- [2] J.-S. Chou and N.-S. Truong, "Cloud forecasting system for monitoring and alerting of energy use by home appliances," *Applied Energy*, Vol. 249, pp. 166–177, Sep. 2019, <https://doi.org/10.1016/j.apenergy.2019.04.063>
- [3] G.-F. Angelis, C. Timplalexis, S. Krinidis, D. Ioannidis, and D. Tzovaras, "NILM applications: Literature review of learning approaches, recent developments and challenges," *Energy and Buildings*, Vol. 261, p. 111951, Apr. 2022, <https://doi.org/10.1016/j.enbuild.2022.111951>
- [4] G. Zheng et al., "DRN: A deep reinforcement learning framework for news recommendation," in *Proceedings of the 2018 World Wide Web Conference*, pp. 167–176, 2018.
- [5] C. Yang et al., "A barking emotion recognition method based on Mamba and Synchrosqueezing Short-Time Fourier Transform," *Expert Systems with Applications*, Vol. 258, p. 125213, Dec. 2024, <https://doi.org/10.1016/j.eswa.2024.125213>
- [6] Q. Sun, M. Pickett, A. K. Nain, and L. Jones, "Transformer layers as painters," *Proceedings of the AAAI Conference on Artificial Intelligence*, Vol. 39, No. 24, pp. 25219–25227, Apr. 2025, <https://doi.org/10.1609/aaai.v39i24.34708>
- [7] E. L. de Aguiar, L. Da Silva Nolasco, A. E. Lazzaretti, D. R. Pipa, and H. S. Lopes, "St-nilm: A wavelet scattering-based architecture for feature extraction and multilabel classification in nilm signals," *IEEE*

Sensors Journal, Vol. 24, No. 7, pp. 10540–10550, Apr. 2024,
<https://doi.org/10.1109/jsen.2024.3360188>

- [8] Y. Xu, X. Huang, X. Zheng, Z. Zeng, and T. Jin, “VMD-ATT-LSTM electricity price prediction based on grey wolf optimization algorithm in electricity markets considering renewable energy,” *Renewable Energy*, Vol. 236, p. 121408, Dec. 2024, <https://doi.org/10.1016/j.renene.2024.121408>
- [9] I. Jrhilifa, H. Ouadi, A. Jilbab, S. Gheouany, N. Mounir, and S. El Bakali, “Vmd-gru based non-intrusive load monitoring for home energy management system,” *IFAC-PapersOnLine*, Vol. 58, No. 13, pp. 176–181, Jan. 2024, <https://doi.org/10.1016/j.ifacol.2024.07.479>
- [10] S. G. Padder et al., “Data-driven approaches for estimation of EV battery SoC and SoH: A review,” *IEEE Access*, Vol. 13, pp. 35048–35067, Jan. 2025, <https://doi.org/10.1109/access.2025.3539528>
- [11] W. Wu et al., “A Transformer-BiLSTM-MLP model for SOC estimation of lithium-ion batteries,” *Journal of Energy Storage*, Vol. 126, p. 116815, Aug. 2025, <https://doi.org/10.1016/j.est.2025.116815>
- [12] T. L. Young, J. Gopsill, M. Valero, S. Eikevåg, and B. Hicks, “Comparing four machine learning algorithms for household non-intrusive load monitoring,” *Energy and AI*, Vol. 17, p. 100384, Sep. 2024, <https://doi.org/10.1016/j.eyai.2024.100384>
- [13] K. Thirunavukkarasu and L. Raju, “Enhanced energy efficiency smart buildings through LoRaWAN and adaptive machine learning techniques,” *Wireless Networks*, Vol. 31, No. 3, pp. 2875–2892, Feb. 2025, <https://doi.org/10.1007/s11276-025-03915-5>
- [14] I. Khalil, A. Daghour, M. A. Chanoui, Z. Guennoun, and A. Addaim, “Energy-efficient deep learning for cloud detection onboard nanosatellite,” *IEEE Journal of Selected Topics in Applied Earth Observations and Remote Sensing*, Vol. 18, pp. 9968–9985, Jan. 2025, <https://doi.org/10.1109/jstars.2025.3553304>
- [15] D. Kumar and U. Satija, “Optimized EEG multi-noise removal and compression: deploying a PbP-QLP enhanced autoencoder on STM32 microcontroller,” *IEEE Transactions on Consumer Electronics*, Vol. 71, No. 2, pp. 3218–3228, May 2025, <https://doi.org/10.1109/tce.2025.3562388>
- [16] S. M. S. Anwar, D. Pal, S. Mukhopadhyay, and R. Gupta, “A lightweight method of myocardial infarction detection and localization from single lead ECG features using machine learning approach,” *IEEE Sensors Letters*, Vol. 8, No. 4, pp. 1–4, Apr. 2024, <https://doi.org/10.1109/lens.2024.3374790>
- [17] O. Munoz et al., “Design and implementation of an automatic and self-adaptive NILM system using unsupervised learning and an IoT platform,” *Electric Power Systems Research*, Vol. 241, p. 111376, Apr. 2025, <https://doi.org/10.1016/j.epsr.2024.111376>
- [18] S. Kannimuthu, A. Sidhu, P. Chandrakala, Y. Parmar, S. B. Sollapur, and A. Ingle, “Enhancing watershed segmentation for precise mammogram detection and classification with the application of feedforward neural network strategies,” in *2024 IEEE 4th International Conference on ICT in Business Industry and Government (ICTBIG)*, pp. 1–6, 2024, <https://doi.org/10.1109/ictbig64922.2024.10911243>
- [19] M. Dheer, S. B. Sollapur, and M. K. Sharma, “Investigating the security considerations of interactive communication media algorithms for networking applications,” in *2024 15th International Conference on Computing Communication and Networking Technologies (ICCCNT)*, pp. 1–6, 2024, <https://doi.org/10.1109/icccnt61001.2024.10725810>
- [20] S. S. B., S. R. Suryawanshi, M. M. S., D. K. Dond, G. Chate, and A. Bhowmik, “Predictive modeling of tool life in turning using ANN-Taguchi hybridization,” *The Scientific World Journal*, Vol. 2024, No. 1, 2024, <https://doi.org/10.1155/2024/9129669>
- [21] F. Ahmed, M. H. I. Bijoy, H. R. Hemal, and S. R. H. Noori, “Smart aquaculture analytics: enhancing shrimp farming in Bangladesh through real-time IoT monitoring and predictive machine learning analysis,” *Heliyon*, Vol. 10, No. 17, p. e37330, Sep. 2024, <https://doi.org/10.1016/j.heliyon.2024.e37330>



Xihuan Su graduated from Guangdong University of Technology, China, with a master’s degree in mechanical engineering in 2018. He is currently an international doctoral student in Electronic Engineering at Batangas State University, a national engineering university in the Philippines. His research focuses on signal processing, Machine Learning, and Intelligent Systems.



Dr. **Antonette V. Chua** is an Associate Professor II and the Graduate School Program Coordinator at Batangas State University, The National Engineering University. She earned her Doctor of Philosophy in Electronics Engineering and Master of Science in Electronics and Communications Engineering from Batangas State University, and her Bachelor of Science in Electronics and Communications Engineering from Southern Luzon State University. She is a licensed Electronics Engineer and an active Board Director of the Institute of Electronics Engineers of the Philippines (IECEP) – Batangas Chapter. Dr. Chua has been involved in various research initiatives, including the CHED IDIG Project on the Straight Program in Electronics Engineering and the HUGIS Project on Harmonized and Unified GIS for Industry Productivity. She is the Vice Governor for Education of the Institute of Electronics Engineers of the Philippines – Batangas Chapter for 2025 and has served in different positions in the organization since 2014. Her research interests include Natural Language Processing, Machine Learning, and Intelligent Systems.



Anton Louise De Ocampo, after earning his B.S. in Electronics and Communications Engineering (BSECE) degree in De La Salle Lipa in 2007, pursued M.S. and Ph.D. degrees in Electronics and Communications Engineering at De La Salle University (DLSU) and graduated in 2016 and 2020 respectively. He is an Associate Professor in the Department of Electronics Engineering at Batangas State University – The National Engineering University and the head of the Digital Transformation Center at the same university. His research interests include machine learning, image processing, and algorithm development applied to environmental characterization. He worked on projects related to image processing and machine learning applications in smart agriculture. (Based on a document published on 19 December 2024).



Ralph Gerard B. Sangalang received his B.S. degree in electronics and communications engineering and M.S. in electronics engineering at Batangas State University, Philippines. He obtained the Ph.D. in electrical engineering and the Ph.D. in electronics engineering under the double degree program at National Sun Yat-Sen University in Taiwan and Batangas State University, The National Engineering University in the Philippines in 2023 and 2024, respectively. He was awarded the Yeh Kung-Chie Memorial Scholarship Award at NSYSU in 2023. He is an Associate Professor and Head of the Electronic Systems Research Center, and currently serves as the Program Chair of the Electronics Engineering Graduate programs at Batangas State University – TNEU. He is responsible for overseeing the Master of Science, Master of Engineering, and Doctor of Philosophy programs in the field of electronics engineering. He was the Program Chair of BS Electronics Engineering during 2017-2021 and Interim Program Chair of the BS Biomedical Engineering. He was also formerly the Student Outcome Committee Chair of the College of Engineering, Architecture and Fine Arts from 2014-2021. He is the Governor of the Institute of Electronics Engineers of the Philippines – Batangas Chapter for 2025 and has served in different positions in the organization since 2014. He is also the Vice-President for Technical of the Mechatronics and Robotics Society of the Philippines- Batangas Chapter. He has served as reviewer in ISCAS, AICAS, ISCAIE, ISBI, CSSP, IJE, Kybernetika, and IJCDS. His research interests include memory design, AI circuits, digital systems, control systems, computational modeling, fractional circuits, research security, fractional systems, and engineering education.



Oliver Lexter July Alvarez Jose earned his Ph.D. in electrical engineering from the National Sun Yat-sen University, Kaohsiung, Taiwan, in January 2024, and Ph.D. in Electronics Engineering from Batangas State University (BatState-U) - TNEU, Batangas City, Philippines, in July 2024. Dr. Jose has been a faculty member under the Department of Electronics Engineering at BatState-U-TNEU since 2012. From May to December 2016, he served as a Product Engineer in the Automation Department at Cypress Manufacturing Ltd., Cavite, Philippines. In 2024, Dr. Jose became the Program Chair of Biomedical Engineering, BatState-U -TNEU. His research interests include. DPWM techniques circuit design, active gate drivers for power MOS, and logic circuit design.



Dianyou Kang graduated from Guangdong University of Technology in China in 2015 with a Master's degree in mechanical engineering. He is currently an international doctoral student majoring in Electronic Engineering at Batangas State University, National University of Engineering, Philippines. His research focuses on artificial intelligence and machine learning.